RECONSTRUCTION OF COMPLEX REFRACTIVE-INDEX DISTRIBUTIONS USING MODIFIED NEWTON-KANTOROVICH METHOD

Haruyuki HARADA[†], Mitsuru TANAKA[††], Takashi TAKENAKA[†††] and Hironori GOTO[††]

[†] Division of Computer Center, Nippon Bunri University, Oita-shi, 870-03 Japan

[††] Department of Electrical and Electronic Engineering, Oita University, Oita-shi, 870-11 Japan

[†††] Department of Electrical Engineering and Computer Science, Nagasaki University, Nagasaki-shi, 852 Japan

1. Introduction

For electromagnetic characterization of scatterers, several reconstruction algorithms have been proposed to determine the size, shape, and electromagnetic properties of an object[(1)-(4)]. The conventional diffraction tomography techniques within the first-order Born or Rytov approximation are applicable to weakly diffracting objects[(1)]. Recently, practical methods of image reconstruction have been presented for a wide range of situations where the two approximations break down[(2),(3)]. However, a regularization technique has been utilized in the inverse procedure to circumvent ill-posedness of the problem.

This paper describes a method for reconstructing a lossy dielectric cylinder from the knowledge of an incident field and the resulting scattered far-field. The two-dimensional object is assumed to be located in a lossless and homogeneous dielectric medium. The inverse scattering problem requires us to solve a nonlinear integral equation for an object function f, which is a function of complex refractive index of the object. Applying the modified Newton-Kantorovich method[(5)] to the integral equation, one can obtain an iterative formula for getting the pth estimate of f without employing regularization methods. Computer simulations are performed for a homogeneous circular cylinder and a stratified cylinder consisting of two concentric homogeneous layers. From the simulated results, we can conclude that the present procedure provides high-quality reconstructions even for cases where the first-order Born approximation fails. The results also demonstrate fast convergence properties of the algorithm.

2. Formulation

Consider a lossy dielectric cylinder of refractive index $n_s(x,y)$ illuminated by a TM-polarized plane wave. Figure 1 illustrates the geometrical configuration of the problem. Note that the object with cross section Ω is invariant along the z-direction and that the surrounding dielectric medium is lossless and homogeneous. The scatterer is characterized by the complex object function

$$f(x,y)=k_0^2[n_s^2(x,y)-n^2], \tag{1}$$

where k_0 and n denote the wavenumber of free space and the refractive index of the external medium, respectively. The scattered field data is measured along a semicircle C ($\theta-\pi\le\phi\le\theta$) of very large radius r.

The inverse scattering problem discussed here is reduced to a nonlinear integral equation for f[(4)]. The inversion of the integral equation can be derived using the modified Newton-Kantorovich method[(5)]. Then we get

$$\mathbf{L}_{f_0}(f_{p+1}(x,y)-f_p(x,y))=-\mathbf{A}f_p(x,y), \qquad p=0,1,2,\cdots. \tag{2}$$

Here f_p denotes the pth estimate of f, $\mathbf{A}$ indicates a nonlinear integral operator[4], and $\mathbf{L}_{f_0}$ is the Fréchet derivative of $\mathbf{A}$ at an initial guess f_0. It should be remarked that $\mathbf{L}_{f_0}$ is a linear operator. Substituting the expression for the Fréchet derivative[6] into Eq. (2), we can obtain an iterative formula for getting f_{p+1} from f_p. Since the formula is an integral equation for f_{p+1} of the first kind, its solution has the properties of nonuniqueness and numerical instability. If an initial guess f_0 is set to zero, however, we do not require any regularization method to circumvent ill-posedness of the problem. Then the integral equation may be now written as[4]

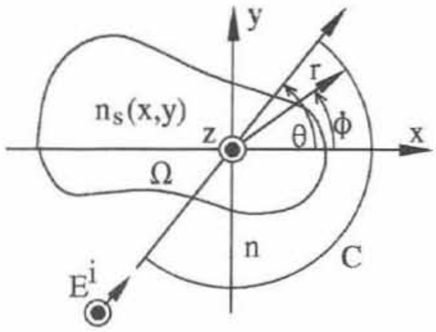

Figure 1. Geometrical configuration of the problem.

$$F_{p+1}(\alpha, \beta) = \int_\Omega f_{p+1}(x, y) \exp[j(\alpha x + \beta y)] dx\, dy$$

$$= W(\theta;\phi) - \int_\Omega f_p(x, y) \left[\frac{E^t(f_p; \theta; x, y)}{E^i(\theta; x, y)} - 1 \right] \exp[j(\alpha x + \beta y)] dx\, dy, \qquad (3)$$

where

$$\alpha = nk_0(\cos\phi - \cos\theta), \qquad (4a)$$

$$\beta = nk_0(\sin\phi - \sin\theta), \qquad (4b)$$

$$\theta - \pi \leq \phi \leq \theta. \qquad (4c)$$

In Eq. (3), $W(\theta;\phi)$ characterizes the directional pattern of the scattered far-field[4], $E^i(\theta; x,y)$ is the incident electric field, and $E^t(f_p; \theta; x,y)$ is a total electric field. Note that the total field can be obtained by solving the direct scattering problem. For numerical calculation of $E^t(f_p; \theta; x,y)$, the moment method and the FFT-CG method[7] are utilized. Then the execution time and the storage on a computer are remarkably reduced. From Eq. (3), one can obtain f_{p+1} by performing the inverse Fourier transform of its spectrum F_{p+1}. As is evident from Eqs. (4a) and (4b), F_{p+1} is bandlimited within the disk D of radius $2nk_0$ with center at the origin when θ varies from 0 to 2π and ϕ from $\theta-\pi$ to θ. Thus f_{p+1} can be successfully recovered without employing regularization methods.

3. Simulated Results and Discussion

For some lossy circular cylinders, computer simulations are made to show the validity of our algorithm. The convergent criterion of the relative error[4] is set to 10^{-8}.

Figure 2 illustrates reconstructions of the complex refractive index n_s on the x axis for the homogeneous circular cylinder of radius 1λ and refractive index 1.05–j0.005. Here λ is the wavelength in the surrounding medium, which is now assumed to be free space. In Fig. 2, Re and Im indicate the real part and the imaginary part, respectively. The solid and short-dashed curves, respectively, denote the final convergent solutions after 17 iterations and the results of the first-order Born approximation. The long-and-short dashed curves shown in this figure present the results reconstructed by a low-pass filtered (LPF) version of the true object function[4], i.e., the inverse Fourier transformation of its spectrum whose values outside the disk D are replaced by zero.

Figure 3 shows reconstructed results of n_s on the x axis for the stratified cylinder consisting of two concentric homogeneous layers. Here the radii and the complex refractive indices of the two layers are, respectively, 1λ, 0.5λ, and 1.025–j0.0025, 1.05–j0.005. Note that the final convergent solutions in Fig. 3 are the results from 8th iteration.

Figures 4 and 5 present reconstructions of n_s on the x axis. In Figs. 4 and 5, the true values of $\mathrm{Re}(n_s)$ and the radii are the same as those used in Figs. 2 and 3, respectively. However, the true values of $\mathrm{Im}(n_s)$ are ten times as large as those used in Figs. 2 and 3. The final convergent solutions in Figs. 4 and 5 are the results after 13 and 9 iterations, respectively.

From Figs. 2–5, it is seen that the results of the first-order Born approximation are highly distorted depending on the losses within the objects. However, the accuracy of the reconstructions based on our algorithm is not influenced by the amount of cylinder loss. Furthermore, the reconstructed images show good agreement with the results obtained from the LPF version of the true object function.

4. Conclusions

An efficient procedure for reconstructing a lossy dielectric cylinder has been presented, which is based on the modified Newton-Kantorovich method. The iterative algorithm does not require the usual regularization techniques. From the simulated results for some circular cylinders, it can be concluded that the reconstructed images do not suffer distortion which depends upon the amount of cylinder loss. In addition, the real and imaginary components of the complex indices of refraction can be successfully reconstructed even for cases where the first-order Born approximation fails. Furthermore, the simulated results demonstrate fast convergence properties of the procedure.

References

(1) Kak A. C. and Slaney M. : "Principles of Computerized Tomographic Imaging", pp. 203-273, IEEE Press, New York (1988).
(2) Wang Y. M. and Chew W. C., Int. J. Imaging Syst. & Technol., **1**, pp. 100-108 (1989).
(3) Chew W. C. and Wang Y. M., IEEE Trans. Med. Imaging, **9**, 2, pp. 218-225 (June 1990).
(4) Takenaka T., Harada H. and Tanaka M., Microwave & Optical Technol. Lett., **5**, 2, pp. 94-97 (Feb. 1992).
(5) Kantorovich L. V. and Akilov G. P. : "Functional Analysis", 2nd ed., translated by Silcock H. L., pp. 524-525, Pergamon Press, New York (1982).
(6) Connolly T. J. and Wall D. J. N., Inverse Problems, **6**, 6, pp. 949-966 (Dec. 1990).
(7) Borup D. T. and Gandhi O. P., IEEE Trans. Microwave Theory & Tech., **MTT-33**, 5, pp. 417-419 (May 1985).

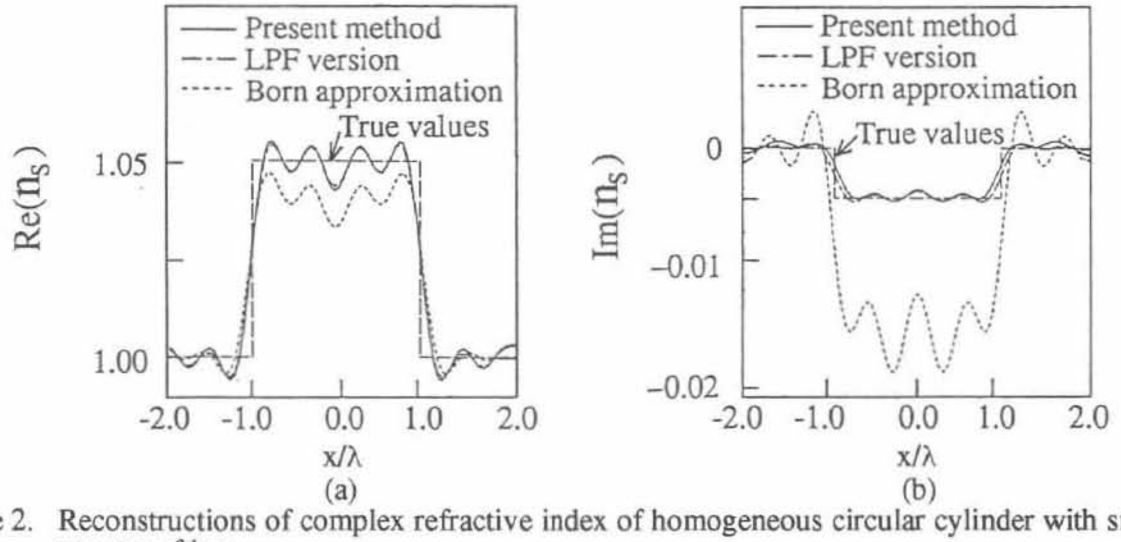

Figure 2. Reconstructions of complex refractive index of homogeneous circular cylinder with small amount of loss.

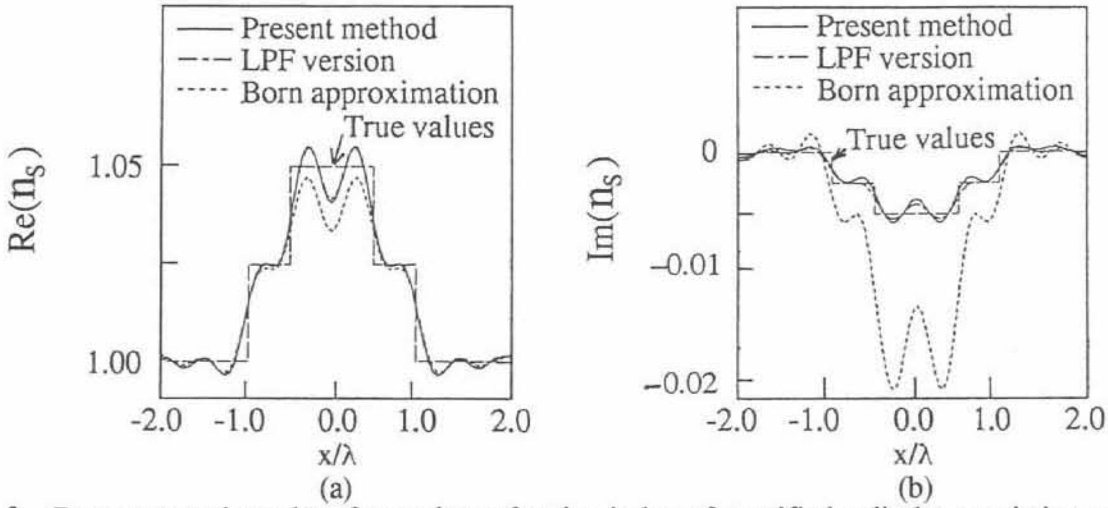

Figure 3. Reconstructed results of complex refractive index of stratified cylinder consisting of two concentric homogeneous layers with small amount of loss.

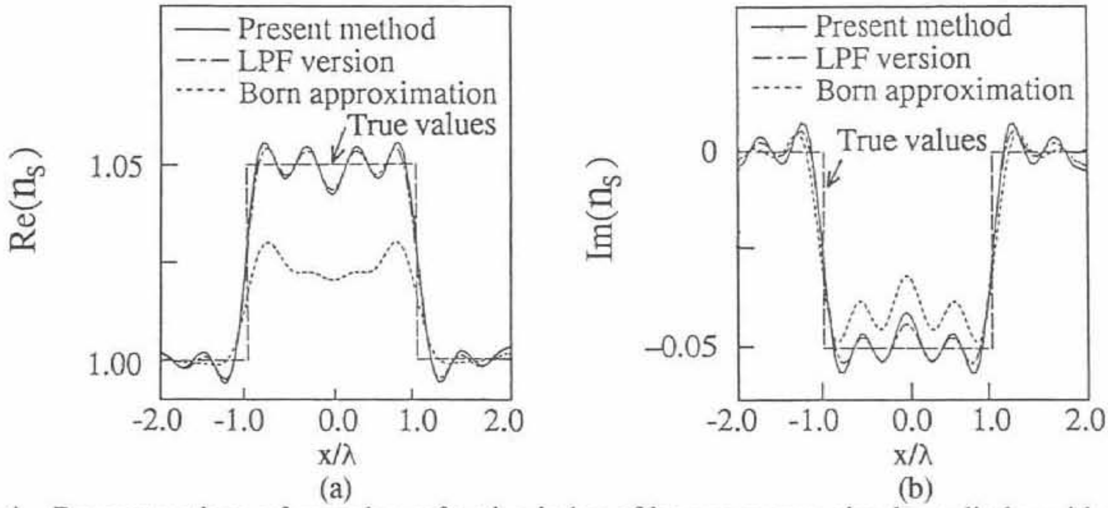

Figure 4. Reconstructions of complex refractive index of homogeneous circular cylinder with large amount of loss.

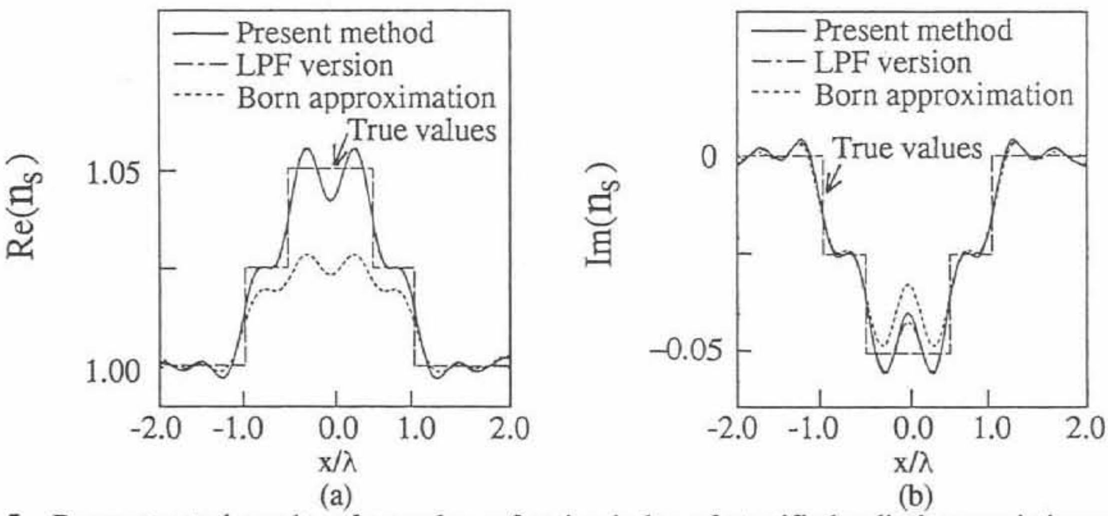

Figure 5. Reconstructed results of complex refractive index of stratified cylinder consisting of two concentric homogeneous layers with large amount of loss.